Original Article
http://dx.doi.org/10.5115/acb.2014.47.1.55
pISSN 2093-3665 eISSN 2093-3673
Anatomy & Cell Biology acb

Topohistology of sympathetic and parasympathetic nerve fibers in branches of the pelvic plexus: an immunohistochemical study using donated elderly cadavers

Nobuyuki Hinata[1], Keisuke Hieda[2], Hiromasa Sasaki[3], Gen Murakami[4], Shinichi Abe[5], Akio Matsubara[2], Hideaki Miyake[1], Masato Fujisawa[1]

[1]Department of Urology, Kobe University Graduate School of Medicine, Kobe, [2]Department of Urology, Hiroshima University School of Medicine, Hiroshima, [3]Division of Gynecology, Ishikawa Prefectural Central Hospital, Kanazawa, [4]Division of Internal Medicine, Iwamizawa Kojin-kai Hospital, Iwamizawa, [5]Department of Anatomy, Tokyo Dental College, Tokyo, Japan

Abstract: Although the pelvic autonomic plexus may be considered a mixture of sympathetic and parasympathetic nerves, little information on its composite fibers is available. Using 10 donated elderly cadavers, we investigated in detail the topohistology of nerve fibers in the posterior part of the periprostatic region in males and the infero-anterior part of the paracolpium in females. Neuronal nitric oxide synthase (nNOS) and vasoactive intestinal polypeptide (VIP) were used as parasympathetic nerve markers, and tyrosine hydroxylase (TH) was used as a marker of sympathetic nerves. In the region examined, nNOS-positive nerves (containing nNOS-positive fibers) were consistently predominant numerically. All fibers positive for these markers appeared to be thin, unmyelinated fibers. Accordingly, the pelvic plexus branches were classified into 5 types: triple-positive mixed nerves (nNOS+, VIP+, TH+, thick myelinated fibers + or −); double-positive mixed nerves (nNOS+, VIP−, TH+, thick myelinated fibers + or −); nerves in arterial walls (nNOS−, VIP+, TH+, thick myelinated fibers−); non-parasympathetic nerves (nNOS−, VIP−, TH+, thick myelinated fibers + or −); (although rare) pure sensory nerve candidates (nNOS−, VIP−, TH−, thick myelinated fibers+). Triple-positive nerves were 5−6 times more numerous in the paracolpium than in the periprostatic region. Usually, the parasympathetic nerve fibers did not occupy a specific site in a nerve, and were intermingled with sympathetic fibers. This morphology might be the result of an "incidentally" adopted nerve fiber route, rather than a target-specific pathway.

Key words: Pelvic autonomic nerve plexus, Neuronal nitric oxide synthase, Vasoactive intestinal polypeptide, Tyrosine hydroxylase, Human anatomy

Received November 2, 2013; Accepted November 13, 2013

Introduction

Immunohistochemistry has long been applied for research on pelvic nerves. Immunohistochemical discrimination between the sympathetic and parasympathetic nerves in the human pelvic plexus or its branches has usually been performed using specimens surgically removed from human adults [1-6] or fetuses [7, 8]. Butler-Manuel et al. [3, 4]

Corresponding author:
Nobuyuki Hinata
Department of Urology, Kobe University Graduate School of Medicine, 7-5-1, Kusunoki-cho, Kobe, Japan
Tel: +81-78-382-6155, Fax: +81-78-382-6169, E-mail: hinata@med.kobe-u.ac.jp

provided particularly elegant photos of the upper part of the pelvic plexus near the sacral promontory after various types of immunostaining. However, the use of surgical specimens does not allow staining of large areas including multiple organs. Small sections make it difficult to obtain an overall picture of the topographical anatomy. In contrast, studies using donated cadavers allow investigation of large areas such as that extending from the urethra to the rectum, but very few such studies have been reported [9-12], possibly because of difficulties with immunostaining. However, Takenaka et al. [10] and Imai et al. [11] were concerned mainly with variations in ganglion cell morphology, and paid no attention to nerve fibers. Ali et al. [9] demonstrated tyrosine hydroxylase (TH)-positive sympathetic nerves directed to the prostate using small sections. To our knowledge, the study by Hieda et al. [12] using immunohistochemistry for neuronal

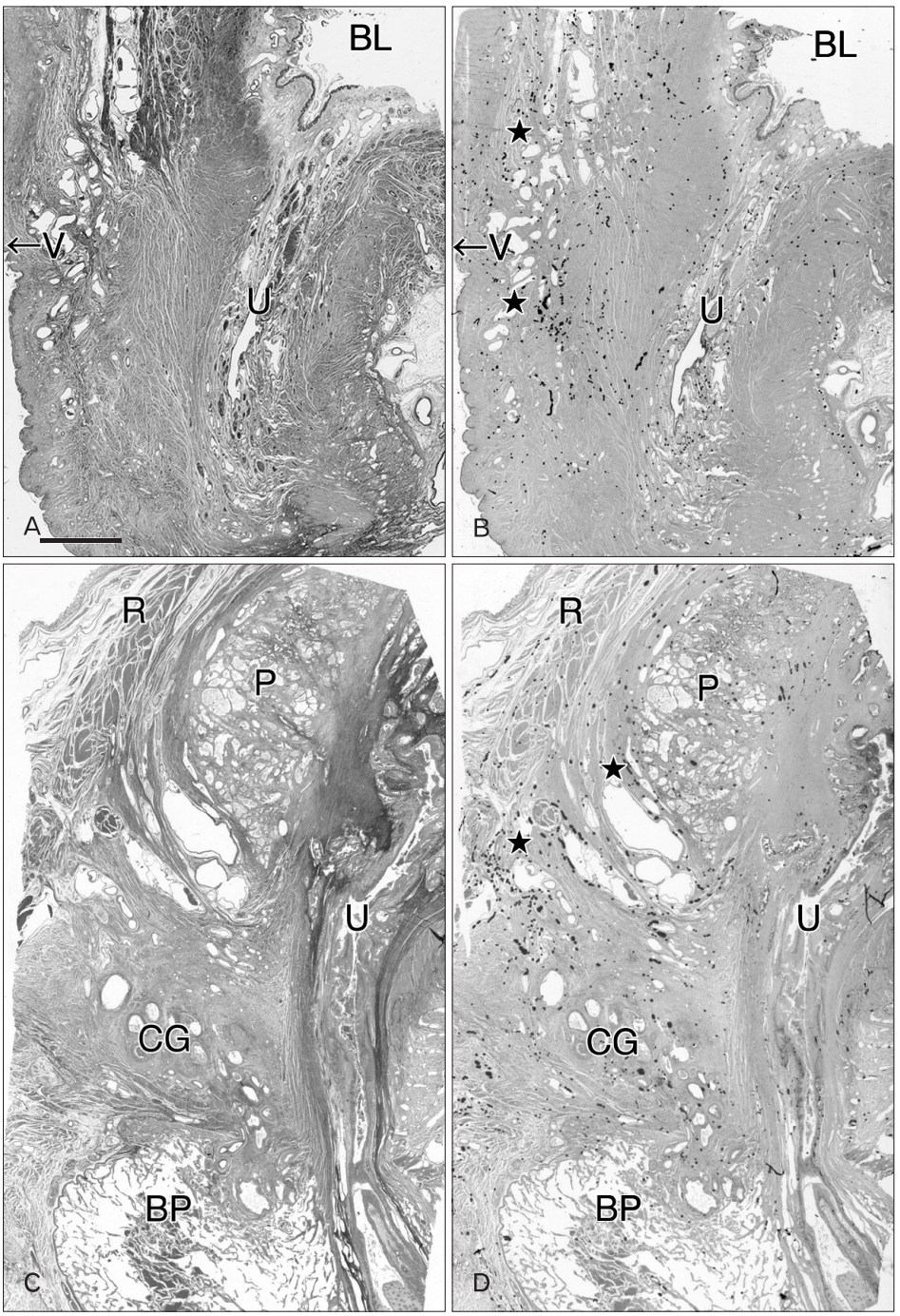

Fig. 1. Topohistology of target regions for the present immunohistochemistry. Panels (A) and (B) (or C and D) are adjacent sagittal sections. Panels (A) and (C) exhibit elastica-Masson staining, while panels (B) and (D) display nerve mapping according to immunohistchemistry of S100. Panels (A) and (B) (a 91-year-old woman) include the bladder (BL), urethra (U) and vagina (V), while panels (C) and (D) (an 88-year-old man) includes the urethra, prostate (P) and rectum (R). We examined topohistology of sympathetic and parasympathetic nerve fibers in the posterior periprostatic region as well as in the infero-anterior part of the paracolpium in females (stars in panels B and D). Panel (B) (or D) contains 385 (or 498) nerves. BP, bulbus penis; CG, Cowper's gland. All panels were prepared at the same magnification. Scale bar in panel (A)=10 mm (A–D).

nitric oxide synthase (nNOS) and TH seems to be a rare example of an attempt to investigate pelvic sympathetic and parasympathetic nerve fibers using large sections.

There have been many excellent studies on the gross anatomy of the pelvic autonomic nerve plexus and its branches [13-17]. However, in the elegant photos presented, showing a network of pelvic nerves, it was not possible to differentiate nerve fibers into sympathetic and parasympathetic types. Therefore it has remained unclear whether all nerves carry both sympathetic and parasympathetic nerve fibers, or whether some nerves carry only a single type. There are also no details of the topohistology of the sympathetic and parasympathetic nerve fibers in a single nerve. Both nNOS and vasoactive intestinal polypeptide (VIP) are known to be expressed in nerve fibers of the pelvic plexus branches, and therefore both have been used as parasympathetic nerve markers [1-4, 18]. However, it is still unclear whether the parasympathetic fibers are bundled and separated from TH-positive sympathetic fibers in a nerve, or whether they are intermingled. There is also limited information about the distribution of periprostatic ganglion cells [10]: according to them, VIP-positive neurons occupy one side and TH-positive neurons the other.

Consequently, to provide a better understanding of pelvic nerve configuration, the present study was conducted to investigate the topohistology of three types of pelvic nerve fibers (nNOS-positive, VIP-positive and TH-positive fibers) in 1) the posterior part of the periprostatic region, including nerves between the prostate and rectum in males, and 2) the infero-anterior part of the paracolpium or paravaginal region in females. Abundant distal branches of the pelvic plexus run through both regions, and these are likely to include both the cavernous nerve and nerves to the urethral sphincters [19-21].

Materials and Methods

The study was performed in accordance with the provisions of the Declaration of Helsinki 1995 (as revised in Edinburgh 2000). We examined 10 donated human cadavers (5 men and 5 women) ranging in age from 73 to 95 years, with a mean age of 85 years. The cause of death had been ischemic heart failure or intracranial bleeding, and we ensured that none of the individuals examined had undergone abdominal surgery during life by examination of medical records as well as macroscopic observation after opening of the abdominopelvic cavity. These cadavers had been donated to Tokyo Dental College for research and education on human anatomy, and their use for research had been approved by the college ethics committee.

The donated cadavers had been fixed by arterial perfusion of 10% v/v formalin solution and stored in 50% v/v ethanol solution for more than 3 months. From one cadaver, we prepared one large tissue block including the bladder, urethra, prostate, uterus, vagina, rectum, and any connective tissue around these viscera. Five to seven slices (15 mm in thickness) were made from one of the hemiblocks after bisection along the midsagittal line, and the specimens were subjected to routine procedures for paraffin-embedded histology. Five to seven large sagittal or frontal slices (70×50 mm) stained with hematoxylin and eosin (H&E) were prepared at 2–3-mm intervals from each of the macro slices. After observation of the large sections to find the desired target regions, we prepared usual-sized sections (50×20 mm) for immunohistochemistry near the former plane. From one paraffin block containing a 15-mm-thick slice, we prepared 2−5 large sections and 8−20 usual-sized sections.

Most sections were stained with H&E and some were used for immunohistochemistry and elastica-Masson staining (a variation of Masson-Goldner staining) [22, 23]. As reported by Hieda et al. [12], the primary antibodies used for nerve immunohistochemistry were 1) mouse monoclonal anti-human S100 protein (1:200, Dako Z0311, Dako, Glostrup, Denmark), 2) rabbit polyclonal anti-human nNOS (1:200, Cell Signaling Technology, Beverly, MA, USA), 3) mouse monoclonal anti-human VIP (1:100, sc25347, Santa Cruz Biotechnology, Santa Cruz, CA, USA), and 4) rabbit polyclonal anti-human TH (1:500, ab152, Millipore-Chemicon, Temecula, CA, USA). We attempted in principle to perform these 4 types of immunohistochemical staining on adjacent sections, but sometimes it was necessary to use near (not adjacent) sections in cases where immunostaining or section preparation was unsuccessful. The secondary antibody was labeled with horseradish peroxidase (HRP), and antigen-antibody reactions were detected by the HRP-catalyzed reaction with diaminobenzidine. Counterstaining with hematoxylin was performed on the same samples. A negative control lacking the primary antibody was set up for each of the specimens. Observations and photography were usually performed with a Nikon Eclipse 80 (Nikon, Tokyo, Japan), but photos at ultra-low magnification (with an objective lens of less than ×1) were taken using an Epson GTX970 (Epson, Tokyo, Japan) high-grade flat scanner with

http://dx.doi.org/10.5115/acb.2014.47.1.55

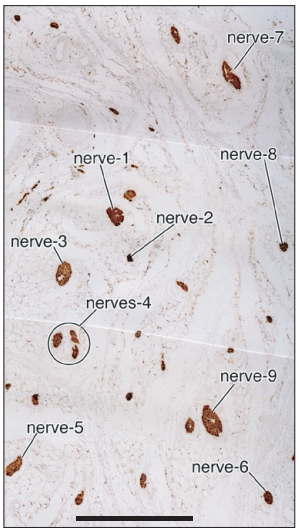

Fig. 2. Nerve distribution in the antero-inferior part of the paracolpium. S100 immunohistochemistry. Frontal section. A specimen from an 88-year-old-woman. Composite nerve fibers of the numbered nerves (nerve-1, -2, -3, -4, -5, -6, -7, -8, and -9) will be shown in Figs. 3–5. Scale bar=1 mm.

translucent illumination.

Results

In 3 of the 10 cadavers (2 men and 1 woman), in entire sectional areas larger than the posterior periprostatic region or the lower paravaginal region (Fig. 1), we counted "nerves containing nNOS-positive fibers" (hereafter referred to as "nNOS-positive nerves"). In the woman (aged 91 years), the section contained 385 nerves and more than half of them (205 nerves) expressed nNOS. Likewise, nNOS-positive nerves were numerically predominant in the infero-anterior part of the paracolpium (Fig. 2). In the 2 men (aged 88 and 95 years), they contained 498 and 520 nerves, among which 364 and 385 were nNOS-positive, respectively. Although we did not perform a count, nNOS-positive nerves were a major population among pelvic plexus branches in sections from the

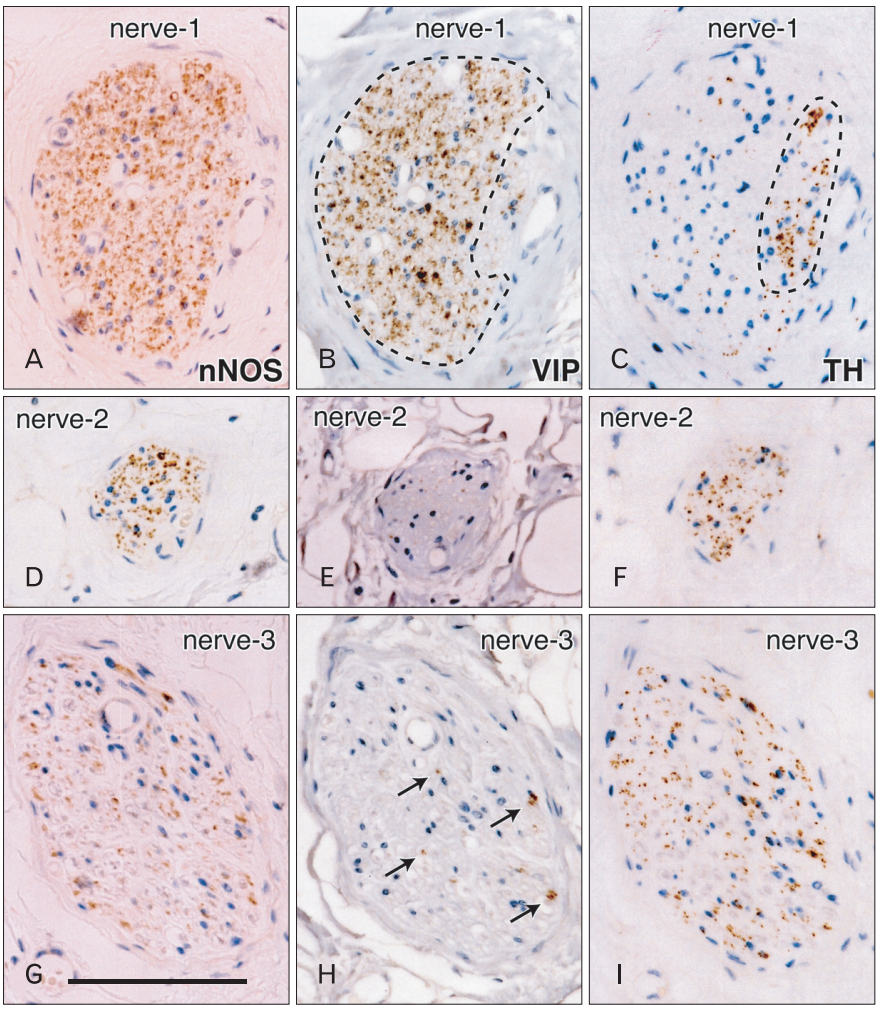

Fig. 3. Sympathetic and parasympathetic nerve fibers in the paravaginal nerves-I. Topographical relation among the nerves-1, -2, -3 was shown in Fig. 2. The parasympathetic nerve markers are neuronal nitric oxide synthase (nNOS) and vasoactive intestinal polypeptide (VIP), while the sympathetic marker is tyrosine hydroxylase (TH). The left-hand side column displays immunohistochemistry of nNOS, the middle column shows that of VIP and the right-hand side column exhibits that of TH. (A–C) Nerve-1 is rich in nNOS- and VIP-positive nerve fibers: the area of the latter fibers (VIP) appears not to contain TH-positive fibers (encircled by dotted line in panels B and C). (D–F) Nerve-2 is negative for VIP. (G–I) Nerve-3 contains a few VIP-positive nerve fibers (arrows in panel H). These results are summarized in Table 1. All panels were prepared at the same magnification. Scale bar in panel (G)=0.1 mm (A–I).

other 2 male cadavers. All of the NOS-, VIP- and TH-positive fibers were thin and appeared to be unmyelinated. However, among these nNOS-positive nerves, the features of nerve fiber morphology, such as their number and location in the nerve, differed (see below).

Notably, nearby nerves, even those located adjacently, did not invariably have a similar composition of sympathetic and parasympathetic nerve fibers. The fiber composition of a nerve did not appear to be related to nerve thickness. As an example, Figs. 3–5 demonstrate the composite fibers of nine nerves in an area of about 2×4 mm in the infero-anterior part of the paracolpium: six of the nine nerves were triple-positive (nNOS+, VIP+, TH+) and three were double-positive (nNOS+, VIP−, TH+). Two of the nine nerves contained abundant VIP-positive fibers. Thus, the paravaginal region appeared to be rich in nNOS-positive nerves. In general, the triple-positive nerves accounted for 15–28% of all examined nerves in the lower paracolpium. However, in the posterior periprostatic region, such nerves accounted for less than 5%. Thus, the branches in the female pelvic plexus were characterized by a high content of VIP-positive nerves. Although situated at the medial margin of the regions examined, nerves in the rhabdosphincter area exhibited a double-positive pattern (nNOS+, VIP−, TH+) (Fig. 6B–D). In both genders, nerves without nNOS-positive fibers were seen in two limited areas: 1) thick arterial walls

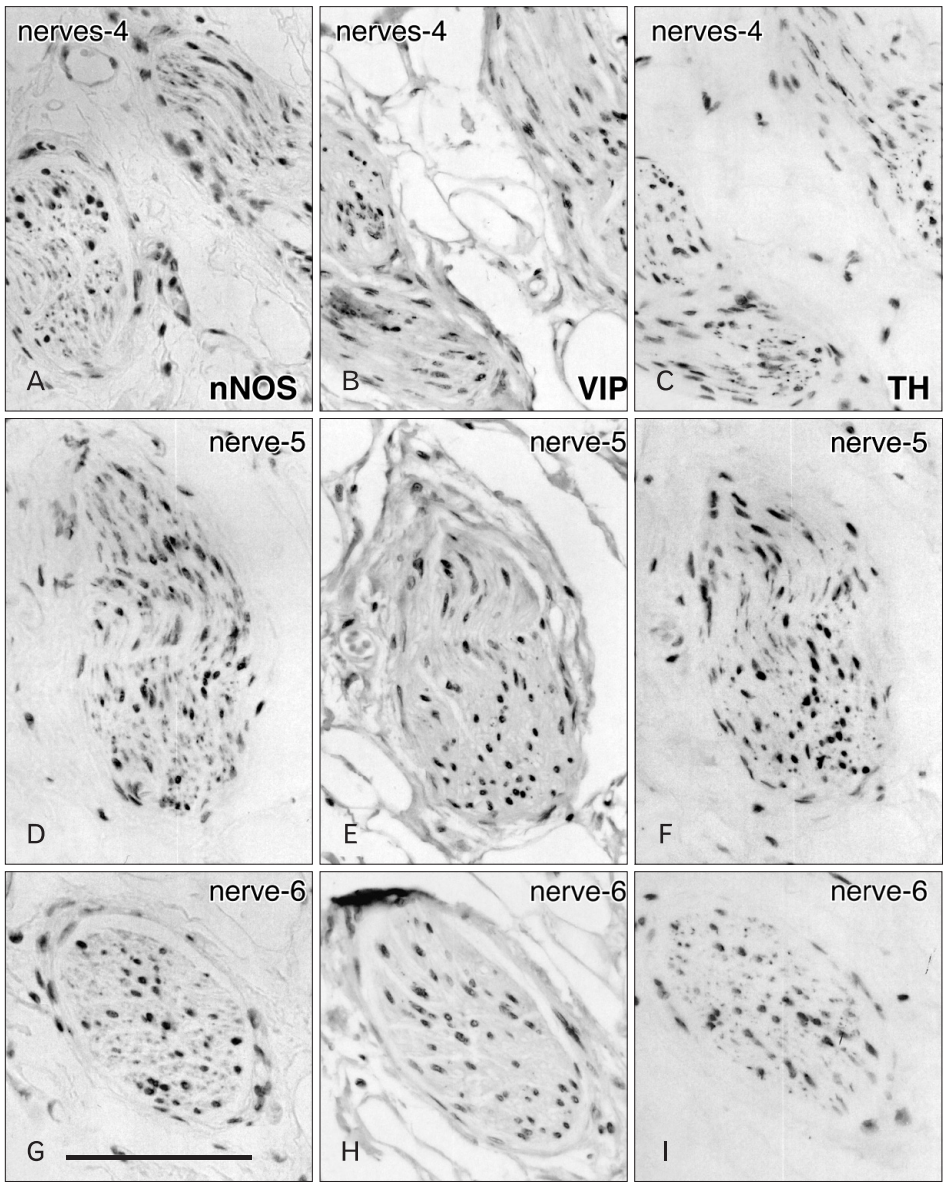

Fig. 4. Sympathetic and parasympathetic nerve fibers in the paravaginal nerves-II. Topographical relation among the nerves-4, -5, -6 was shown in Fig. 2. The left-hand side column displays immunohistochemistry of neuronal nitric oxide synthase (nNOS), the middle column shows that of vasoactive intestinal polypeptide (VIP) and the right-hand side column exhibits that of tyrosine hydroxylase (TH). (A–C) One of nerves-4 does not contain VIP-positive nerve fibers. (D–F) Nerve-5 appears to be negative for VIP. (G–I) Nerve-6 is negative for VIP. These results are summarized in Table 1. All panels were prepared at the same magnification. Scale bar in panel (G)=0.1 mm (A–I).

http://dx.doi.org/10.5115/acb.2014.47.1.55

(Fig. 6E–G) and 2) in and along the levator ani muscle (Fig. 7). With the exception of arterial walls, most of these nerves contained thick myelinated fibers, i.e., likely sensory nerve fibers. Similarly, with a few exceptions in and along the levator ani (Fig. 7G), most of the nerves contained TH-positive sympathetic nerve fibers, irrespective nerve thickness. In addition, although the pudendal nerve was composed of abundant TH-positive fibers and thick myelinated fibers, it did not express either nNOS-positive or VIP-positive fibers in the ischiorectal fossa (VIP, not shown) (Fig. 7K, L). These results are summarized in Table 1.

On the basis of the present observations, at least in the posterior part of the periprostatic region and the infero-anterior part of the paracolpium, the pelvic plexus branches were classifiable into 5 types according to their composite fibers (Table 2): 1) triple-positive mixed nerves (nNOS+, VIP+, TH+, thick myelinated fibers + or −); 2) double-positive mixed nerves (nNOS+, VIP−, TH+, thick myelinated fibers + or −); 3) nerves in arterial walls (nNOS−, VIP+, TH+, thick myelinated fibers−); 4) non-parasympathetic nerves (nNOS−, VIP−, TH+, thick myelinated fibers + or −); and 5) (albeit rare) pure sensory nerve candidates (nNOS−, VIP−, TH−, thick myelinated fibers+). The pudendal nerve in the ischiorectal fossa was a typical example of a non-parasympathetic nerve. Although a fiber type-specific distribution was sometimes observed in some nerves (Figs. 3B, C, 5B–E), sympathetic and parasympathetic fibers were usually intermingled. Consequently, TH-positive sympathetic nerve fibers as well as

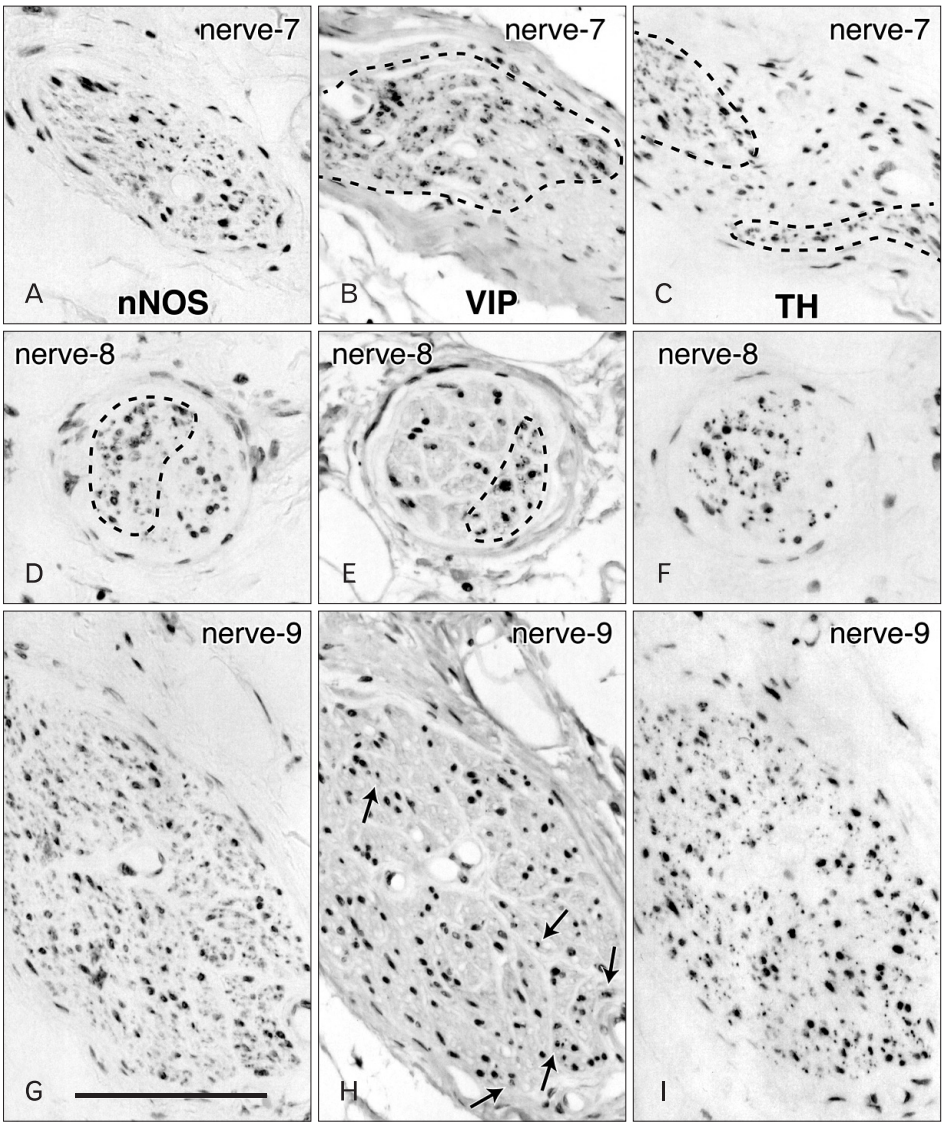

Fig. 5. Sympathetic and parasympathetic nerve fibers in the paravaginal nerves-III. Topographical relation among the nerves-7, -8, -9 was shown in Fig. 2. The left-hand side column displays immunohistochemistry of neuronal nitric oxide synthase (nNOS), the middle column shows that of vasoactive intestinal polypeptide (VIP) and the right-hand side column exhibits that of tyrosine hydroxylase (TH). (A–C) In nerve-7, the area of VIP-positive nerve fibers appears not to contain TH-positive fibers (encircled by dotted line in panels B and C). (D–F) In nerve-8, the area of nNOS-positive nerve fibers appears not to contain VIP-positive fibers (encircled by dotted line in panels D and E). (G–I) Nerve-9 contain a few VIP-positive fibers (arrows in panel H). These results are summarized in Table 1. All panels were prepared at the same magnification. Scale bar in panel (G)=0.1 mm (A–I).

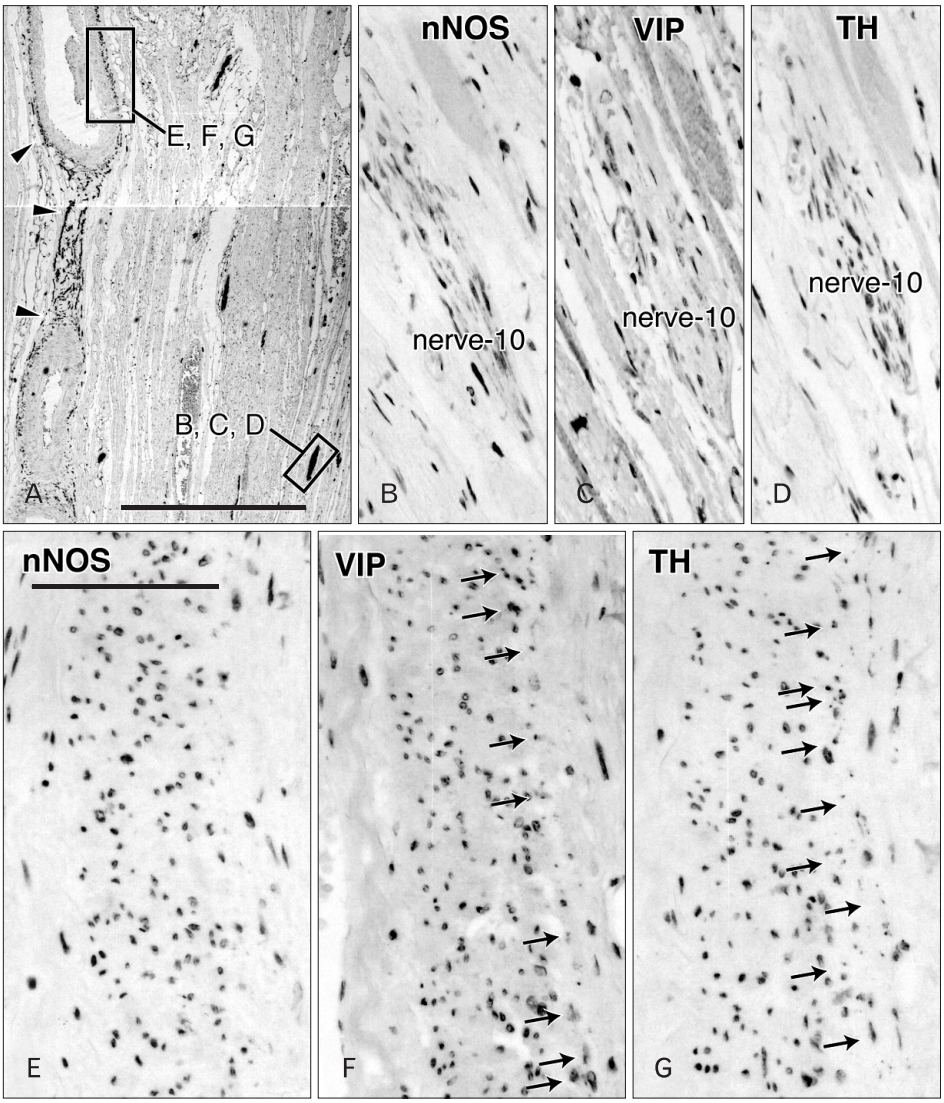

Fig. 6. Sympathetic and parasympathetic nerve fibers in the aortic wall. Frontal section. A specimen from an 88-year-old-woman (the specimen same as in Figs. 2–5). In the anterolateral part of the paracolpium. Panel (A) displays S100 immunohistochemistry: this region contains thick branches of the internal pudendal artery (artery) and a part of the rhabdosphincter. Scale bar=1 mm (A). The striated muscle fibers show false positive reaction with neuronal nitric oxide synthase (nNOS) antibody. Note abundant S100-positive fibers in the arterial wall (arrowheads in panel A). Panels (B), (C), and (D) exhibit a nerve in a square with B, C, D in panel (A). Nerve-10 contains no vasoactive intestinal polypeptide (VIP)-positive fibers. Panels (E), (F), and (G) show nerve fibers in a square with E, F, G in panel (A). The arterial wall contains nNOS-positive fibers as well as tyrosine hydroxylase (TH)-positive fibers (arrows in panel F and G). These results are summarized in Table 1. Panels (B–G) were prepared at the same magnification. Scale bar in panel (E)=0.1 mm (B–G).

thick myelinated sensory fibers appeared to be dominant in the pelvic plexus branches. In contrast to the wide distribution of nNOS-positive parasympathetic fibers, VIP-positive parasympathetic nerve fibers appeared to be restricted to the area near the vagina.

Discussion

Although only limited regions were examined in the present study, we found several patterns of composite fibers in the branches of the pelvic plexus. Using three markers (nNOS, VIP, and TH), the potential combinations of autonomic nerve fibers in the plexus were limited to 4, [nNOS+, VIP+, TH+], [+, −, +], [−, −, +] and [−, −, −], and not 8, which would logically be the largest number (i.e., 2×2×2). The [−, +, +] pattern was not seen in the plexus branches, but only in arterial walls. Neuropeptides including VIP are considered to play a role in secretion from the vaginal wall [24-26]. In particular, VIP-dominant nerve supply to the vagina has been described [1, 25]. The VIP-positive fibers in the female pelvic floor are likely to include sensory fibers [27, 28]. Moreover, it is established that VIP not only acts as a neurotransmitter but also plays a part in neuroprotein, growth regulation and functions as an anti-inflammatory agent [29]. Thus, rich VIP in paravaginal nerves may play a role in nerve repair after mucosal injury of the female genital tract.

Because VIP-positive nerves were much fewer in number than nNOS-positive nerves, we examined the distribution in order to consider the division of nerve branches in the female pelvic plexus. In fact, the branches of the female pelvic plexus

http://dx.doi.org/10.5115/acb.2014.47.1.55

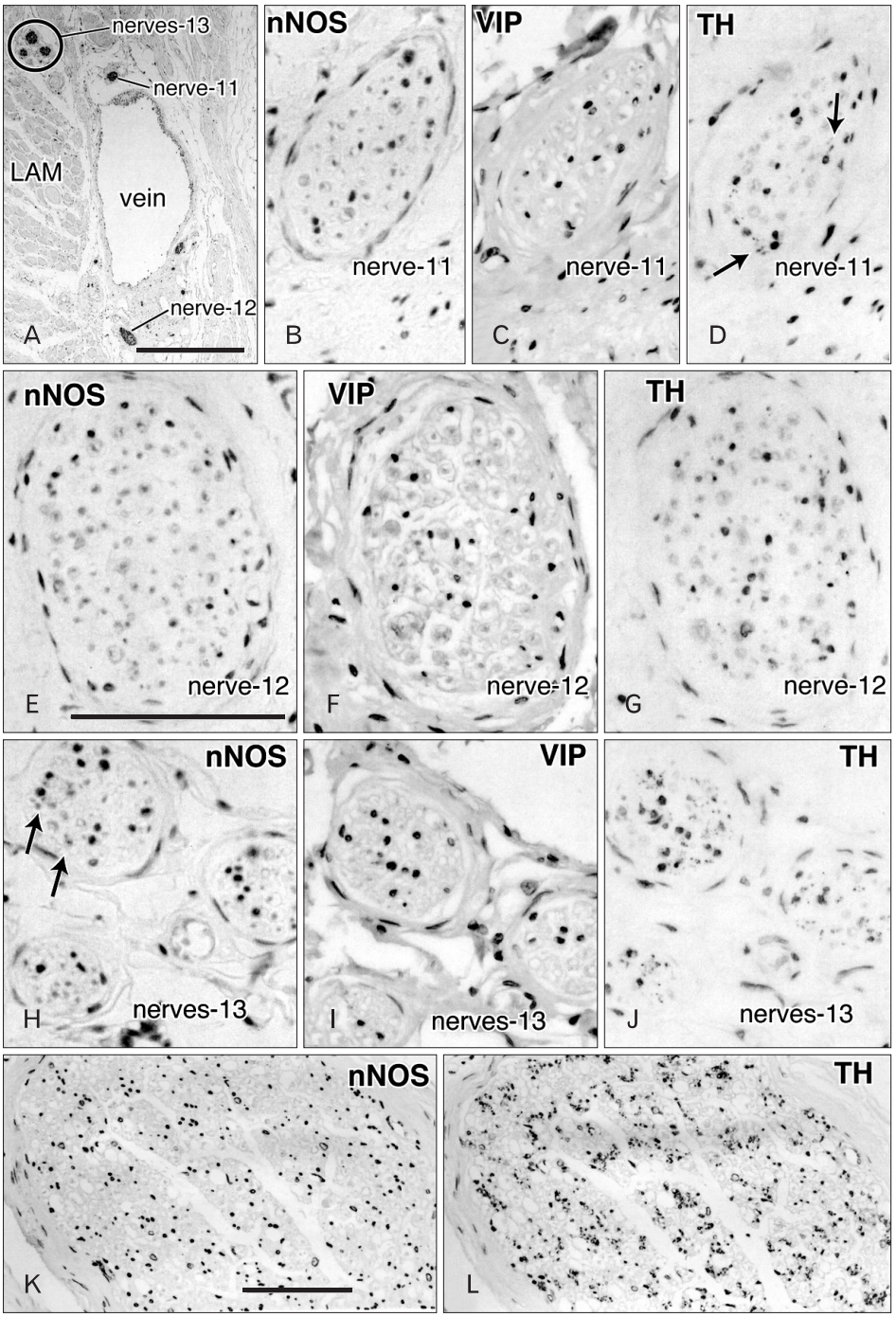

Fig. 7. Sympathetic and parasympathetic nerve fibers along the levator ani muscle. Frontal section. A specimen from an 88-year-old-woman (the specimen same as in Figs. 2–6). Along the levator ani muscle (LAM) in the lateral part of the paracolpium, panel (A) displays nerve distribution using S100 immunohistochemistry. Scale bar=0.5 mm (A). Panels (B), (C), and (D) exhibit nerve-11 in panel (A). This nerve contains a few tyrosine hydroxylase (TH)-positive fibers (arrows). Panels (E), (F), and (G) show nerve-12, a pure sensory nerve candidate. Panels (H), (I), and (J) display TH-single positive nerve-13. In panel (H), brown dots (arrows) appear to be false positive. Panels (K) and (L) exhibit one of multiple nerve bundles of the pudendal nerve in the outside of panel (A). These results are summarized in Table 1. Panels (B–J) (or panels K and L) were prepared at the same magnification. Scale bar in panels (E) and (K)=0.1 mm (B–J), 0.1 mm (K, L). nNOS, neuronal nitric oxide synthase; VIP, vasoactive intestinal polypeptide.

were characterized by their high content of VIP-positive nerves. However, in spite of this network, the adjacent nerves seemed to comprise both VIP-positive and VIP-negative types, suggesting an uneven division of VIP-fibers, perhaps as a result of incidental distribution. Therefore, the intermixing of sympathetic and parasympathetic nerve fibers did not appear to be simple. Nevertheless, most of the plexus branches were double-positive (nNOS+, TH+) and both nNOS-positive and TH-positive fibers seemed to be evenly divided and distributed to all branches. In addition, thick myelinated fibers (candidate sensory nerves) were usually contained in the pelvic plexus branches, although previous studies had reported that their number was limited [30, 31].

There has been no information on the mode of division

of autonomic nerves during fetal development, in contrast to knowledge about somatic nerve branching such as that in the chick lumbar plexus [32-35]. In the developing lumbar nerve plexus, the segmental spinal nerve fibers are distributed to the plexus branches according to strict rules in order to reach their specific skin or muscle target. The pathways chosen by nerve fibers also depend on the route to the flexor or extensor side, as well as the proximal and distal sides of the extremity. Thus, the target-dependent organization of nerve fibers is established so that a bundle of A-muscle nerve fibers occupies one part, whereas a bundle of B-muscle nerve fibers is restricted to another part. Therefore, adjacent nerve branches are most likely to differ in their segmental origin, as well as their targets. However, in many pelvic plexus branches, we were unable to find any fiber type-dependent organization in a nerve, and different types of fibers seemed to be intermingled. The morphology of the pelvic plexus might be a result of "incidental" adoption of a nerve fiber route, rather than a target-specific pathway.

In human fetuses, immunoreactivity for nNOS has been used for identification of the cavernous nerve since the study of Yucel et al. [36]. Using nNOS immunohistochemistry, Alsaid et al. [7] and Moszkowicz et al. [8] provided elegant 3D reconstructions of the fetal cavernous nerves. Their relatively simple reconstructions suggested that the amounts of adult periprostatic nNOS-positive nerves are likely to be underdeveloped. Because of the wide distribution of nNOS-positive nerves along and around the prostate, some researchers have considered that the cavernous nerve in males should form a network along the prostatic surface rather than within a neurovascular bundle [6, 37, 38]. Because these researchers only stained nerves along the prostate, this seemed to facilitate easy identification of the cavernous nerves or their network. Would they have been able to identify cavernous nerves among the number of nNOS-positive nerves identified in the present study? Here we found that nNOS expression was a general characteristic in the pelvic plexus branches, rather than being specific to the cavernous nerve. Although Takenaka et al. [19] demonstrated multiple routes of the cavernous nerves, they did not postulate a network theory. According to them, the cavernous nerve is likely to adopt route "1" among the possible 3 routes. We consider the network theory to be an imagination by urologists who are unaware of the limitations of nNOS as a specific marker of the cavernous nerve.

Table 1. Summary of nerve fiber types in nerves shown in the present figures

	nNOS	VIP	TH	Myelinated fibers
Nerve-1	++	+	+	±
Nerve-2	++	–	++	+
Nerve-3	++	±	++	+
Nerve-4	++	+ or –	+	+
Nerve-5	++	–	++	+
Nerve-6	++	–	++	±
Nerve-7	++	++	+	±
Nerve-8	+	+	++	±
Nerve-9	++	±	++	+
Nerve-10	++	–	++	±
Nerve-11	–	–	±	++
Nerve-12	–	–	–	++
Nerve-13	± or -	–	++	+
Arterial wall*	–	+	+	–
Pudendal nerve†	–	-	++	++

The nerves-1, -2, and -3 are shown in Fig. 3; the nerves-4, -5, and -6 in Fig. 4; the nerves-7, -8, and -9 in Fig. 5; the nerve-10 and "arterial wall" in Fig. 6; and nerves-11, -12, and -13 in Fig. 7. ++, almost 50% or more of all nerve fibers in the nerve; ±, a few fibers. nNOS, neuronal nitric oxide synthase; VIP, vasoactive intestinal polypeptide; TH, tyrosine hydroxylase. *Arterial wall shown in Fig. 6. †Pudendal nerve shown in Fig. 7.

Study limitation

As Hieda et al. [12] reported, nNOS immunohistochemistry is difficult in cadaveric specimens after long preservation. Also, completely quantitative evaluation, such as the percentages of each nerve type, was difficult because of variations in the quality (strong or weak immunoreactions)

Table 2. Basic patterns of combinations of immunoreactivity in pelvic plexus branches

	nNOS-fiber	VIP-fiber	TH-fiber	Myelinated fiber
Triple positive mixed nerves*	Present	Present	Present	Present or absent
Double positive mixed nerves†	Present	Absent	Present	Present or absent
Nerves in arterial walls‡	Absent	Present	Present	Absent
Non-parasympathetic nerves§	Absent	Absent	Present	Present or absent
Pure sensory nerve candidates¶	Absent	Absent	Absent	Present

nNOS, neuronal nitric oxide synthase; VIP, vasoactive intestinal polypeptide; TH, tyrosine hydroxylase. *Typically seen in nerves-1, -4, -7, and -8 (Figs. 3A–C, 4A–C, and 5A–F). †Typically seen in nerves-2, -5, -6, and -10 (Figs. 3D–F, 4D–I, and 6B–D). ‡An example shown in Fig. 6E–G. §Typically seen in nerve-13 (Fig. 7H–J). ¶Seen in nerve-12 (Fig. 7E–G).

http://dx.doi.org/10.5115/acb.2014.47.1.55

of nNOS immunohistochemistry. Although we attempted quantitative estimation, we were unable to rule out the possibility of false negativity in at least 3 cadavers (2 men and 1 woman).

Acknowledgements

We are grateful to the individuals who donated their bodies after death to Tokyo Dental College for research and education on human anatomy without any economic benefit. We also thank their families for agreeing to donate, as well as their patience for the return of their bones after study.

References

1. Hoyle CH, Stones RW, Robson T, Whitley K, Burnstock G. Innervation of vasculature and microvasculature of the human vagina by NOS and neuropeptide-containing nerves. J Anat 1996;188(Pt 3):633-44.
2. Busacchi P, De Giorgio R, Santini D, Bellavia E, Perri T, Oliverio C, Paradisi R, Corinaldesi R, Flamigni C. A histological and immunohistochemical study of neuropeptide containing somatic nerves in the levator ani muscle of women with genitourinary prolapse. Acta Obstet Gynecol Scand 1999;78:2-5.
3. Butler-Manuel SA, Buttery LD, A'Hern RP, Polak JM, Barton DP. Pelvic nerve plexus trauma at radical and simple hysterectomy: a quantitative study of nerve types in the uterine supporting ligaments. J Soc Gynecol Investig 2002;9:47-56.
4. Butler-Manuel SA, Buttery LD, Polak JM, A'Hern R, Barton DP. Autonomic nerve trauma at radical hysterectomy: the nerve content and subtypes within the superficial and deep uterosacral ligaments. Reprod Sci 2008;15:91-6.
5. Uckert S, Stanarius A, Stief CG, Wolf G, Jonas U, Machtens S. Immunocytochemical distribution of nitric oxide synthase in the human seminal vesicle: a light and electron microscopical study. Urol Res 2003;31:262-6.
6. Hisasue S, Hashimoto K, Kobayashi K, Takeuchi M, Kyoda Y, Sato S, Masumori N, Tsukamoto T. Baseline erectile function alters the cavernous nerve quantity and distribution around the prostate. J Urol 2010;184:2062-7.
7. Alsaid B, Bessede T, Karam I, Abd-Alsamad I, Uhl JF, Benoît G, Droupy S, Delmas V. Coexistence of adrenergic and cholinergic nerves in the inferior hypogastric plexus: anatomical and immunohistochemical study with 3D reconstruction in human male fetus. J Anat 2009;214:645-54.
8. Moszkowicz D, Peschaud F, Bessede T, Benoit G, Alsaid B. Internal anal sphincter parasympathetic-nitrergic and sympathetic-adrenergic innervation: a 3-dimensional morphological and functional analysis. Dis Colon Rectum 2012;55:473-81.
9. Ali M, Johnson IP, Hobson J, Mohammadi B, Khan F. Anatomy of the pelvic plexus and innervation of the prostate gland. Clin Anat 2004;17:123-9.
10. Takenaka A, Kawada M, Murakami G, Hisasue S, Tsukamoto T, Fujisawa M. Interindividual variation in distribution of extramural ganglion cells in the male pelvis: a semi-quantitative and immunohistochemical study concerning nerve-sparing pelvic surgery. Eur Urol 2005;48:46-52.
11. Imai K, Furuya K, Kawada M, Kinugasa Y, Omote K, Namiki A, Uchiyama E, Murakami G. Human pelvic extramural ganglion cells: a semiquantitative and immunohistochemical study. Surg Radiol Anat 2006;28:596-605.
12. Hieda K, Cho KH, Arakawa T, Fujimiya M, Murakami G, Matsubara A. Nerves in the intersphincteric space of the human anal canal with special reference to their continuation to the enteric nerve plexus of the rectum. Clin Anat 2013 Mar 20 [Epub]. http://dx.doi.org/10.1002/ca.22227.
13. Maas CP, DeRuiter MC, Kenter GG, Trimbos JB. The inferior hypogastric plexus in gynecologic surgery. J Gynecol Tech 1999;5:55-62.
14. Baader B, Herrmann M. Topography of the pelvic autonomic nervous system and its potential impact on surgical intervention in the pelvis. Clin Anat 2003;16:119-30.
15. Akita K, Sakamoto H, Sato T. Origins and courses of the nervous branches to the male urethral sphincter. Surg Radiol Anat 2003;25:387-92.
16. Costello AJ, Brooks M, Cole OJ. Anatomical studies of the neurovascular bundle and cavernosal nerves. BJU Int 2004;94:1071-6.
17. Mauroy B, Demondion X, Bizet B, Claret A, Mestdagh P, Hurt C. The female inferior hypogastric (= pelvic) plexus: anatomical and radiological description of the plexus and its afferences: applications to pelvic surgery. Surg Radiol Anat 2007;29:55-66.
18. Grozdanovic Z, Baumgarten HG. Colocalisation of NADPH-diaphorase with neuropeptides in the ureterovesical ganglia of humans. Acta Histochem 1996;98:245-53.
19. Takenaka A, Murakami G, Matsubara A, Han SH, Fujisawa M. Variation in course of cavernous nerve with special reference to details of topographic relationships near prostatic apex: histologic study using male cadavers. Urology 2005;65:136-42.
20. Kato M, Niikura H, Yaegashi N, Murakami G, Tatsumi H, Matsubara A. Histotopography of the female cavernous nerve: a study using donated fetuses and adult cadavers. Int Urogynecol J Pelvic Floor Dysfunct 2008;19:1687-95.
21. Hirata E, Koyama M, Murakami G, Ohtsuka A, Abe S, Ide Y, Fujiwara H, Kudo Y. Comparative histological study of levels 1-3 supportive tissues using pelvic floor semiserial sections from elderly nulliparous and multiparous women. J Obstet Gynaecol Res 2011;37:13-23.
22. Motohashi O, Suzuki M, Shida N, Umezawa K, Ohtoh T, Sakurai Y, Yoshimoto T. Subarachnoid haemorrhage induced proliferation of leptomeningeal cells and deposition of extracellular matrices in the arachnoid granulations and subarachnoid space. Immunhistochemical study. Acta Neurochir (Wien) 1995;136:88-91.
23. Hayashi T, Kumasaka T, Mitani K, Yao T, Suda K, Seyama K.

Loss of heterozygosity on tuberous sclerosis complex genes in multifocal micronodular pneumocyte hyperplasia. Mod Pathol 2010;23:1251-60.
24. Boreham MK, Wai CY, Miller RT, Schaffer JI, Word RA. Morphometric properties of the posterior vaginal wall in women with pelvic organ prolapse. Am J Obstet Gynecol 2002;187:1501-8.
25. Hong X, Huang L, Song Y. Role of vasoactive intestinal peptide and pituitary adenylate cyclase activating polypeptide in the vaginal wall of women with stress urinary incontinence and pelvic organ prolapse. Int Urogynecol J Pelvic Floor Dysfunct 2008;19:1151-7.
26. Zhu L, Lang J, Jiang X, Jiang F, Chen J, Wong F. Neuropeptide Y expression in vaginal epithelium of women with pelvic organ prolapse and stress urinary incontinence. Int J Gynaecol Obstet 2008;102:65-8.
27. Maggi CA, Giuliani S, Santicioli P, Patacchini R, Said SI, Theodorsson E, Turini D, Barbanti G, Giachetti A, Meli A. Direct evidence for the involvement of vasoactive intestinal polypeptide in the motor response of the human isolated ileum to capsaicin. Eur J Pharmacol 1990;185:169-78.
28. Jacobson ED, Berguer R, Pawlik WW, Hottenstein OD. Mesenteric purinergic and peptidergic vasodilators. In: Wood JD, editor. The Gastointestinal System. Moltility and Circulation, Handbook of Physiology, Section 6. Bethesda: American Physiological Society; 1989. p.1647-67.
29. Ekblad E, Bauer AJ. Role of vasoactive intestinal peptide and inflammatory mediators in enteric neuronal plasticity. Neurogastroenterol Motil 2004;16 Suppl 1:123-8.
30. Kuntz A, Hoffman H, Schaeffer EM. Fiber components of the splanchnic nerves. Anat Rec 1957;128:139-46.
31. Donker PJ. A study of the myelinated fibres in the branches of the pelvic plexus. Neurourol Urodyn 1986;5:185-202.
32. Lance-Jones C, Landmesser L. Pathway selection by embryonic chick motoneurons in an experimentally altered environment. Proc R Soc Lond B Biol Sci 1981;214:19-52.
33. Honig MG, Lance-Jones C, Landmesser L. The development of sensory projection patterns in embryonic chick hindlimb under experimental conditions. Dev Biol 1986;118:532-48.
34. Ferns MJ, Hollyday M. Motor innervation of dorsoventrally reversed wings in chick/quail chimeric embryos. J Neurosci 1993;13:2463-76.
35. Tosney KW, Hotary KB, Lance-Jones C. Specifying the target identity of motoneurons. Bioessays 1995;17:379-82.
36. Yucel S, De Souza A Jr, Baskin LS. Neuroanatomy of the human female lower urogenital tract. J Urol 2004;172:191-5.
37. Kiyoshima K, Yokomizo A, Yoshida T, Tomita K, Yonemasu H, Nakamura M, Oda Y, Naito S, Hasegawa Y. Anatomical features of periprostatic tissue and its surroundings: a histological analysis of 79 radical retropubic prostatectomy specimens. Jpn J Clin Oncol 2004;34:463-8.
38. Costello AJ, Dowdle BW, Namdarian B, Pedersen J, Murphy DG. Immunohistochemical study of the cavernous nerves in the periprostatic region. BJU Int 2011;107:1210-5.